

**F
O
S
S
E
H
E
N
E
R
G
Y**

DOE/BC/15211-7
(OSTI ID: 761979)

**STABILITY OF MISCIBLE DISPLACEMENTS ACROSS STRATIFIED
POROUS MEDIA**

Topical Report
June 2000

By
Maryam Shariati
Yanis C. Yortsos

Date Published: September 2000

Work Performed Under Contract No. DE-AC26-99BC15211

University of Southern California
Los Angeles, California



**National Petroleum Technology Office
U.S. DEPARTMENT OF ENERGY
Tulsa, Oklahoma**

DISCLAIMER

This report was prepared as an account of work sponsored by an agency of the United States Government. Neither the United States Government nor any agency thereof, nor any of their employees, makes any warranty, expressed or implied, or assumes any legal liability or responsibility for the accuracy, completeness, or usefulness of any information, apparatus, product, or process disclosed, or represents that its use would not infringe privately owned rights. Reference herein to any specific commercial product, process, or service by trade name, trademark, manufacturer, or otherwise does not necessarily constitute or imply its endorsement, recommendation, or favoring by the United States Government or any agency thereof. The views and opinions of authors expressed herein do not necessarily state or reflect those of the United States Government.

This report has been reproduced directly from the best available copy.

DOE/BC/15211-7
Distribution Category UC-122

Stability of Miscible Displacements Across Stratified
Porous Media

By
Maryam Shariati
Yanis C. Yortsos

September 2000

Work Performed Under Contract No DE-AC26-99BC15211

Prepared for
U.S. Department of Energy
Assistant Secretary for Fossil Energy

Thomas B. Reid, Project Manager
National Petroleum Technology Office
P.O. Box 3628
Tulsa, OK 74101

Prepared by
Petroleum Engineering Program
Department of Chemical Engineering
University of Southern California
Los Angeles, CA 90089-1211

TABLE OF CONTENTS

I.	Introduction	1
II.	Formulation	4
	A. Asymptotic analysis at large wavelengths	7
	B. Asymptotic analysis at small wavelengths	10
III.	Numerical Results	10
IV.	A Mechanistic Interpretation.....	12
V.	Effect of Gravity.....	16
VI.	Conclusions	19
	Acknowledgements.....	20
	Figures.....	22-31

I. INTRODUCTION

Porous media are heterogeneous both at the micro-scale (pore-scale) and the macro-scale. Consequently, flow and displacements will be affected by the heterogeneity at both scales. In this paper, we are interested on macro-scale heterogeneity effects. Reflecting their importance, current simulation practices of flow and displacements in porous media are invariably based on heterogeneous permeability fields. Here, we will focus on a specific aspect of such problems, namely the stability of miscible displacements in stratified porous media, where the displacement is perpendicular to the direction of stratification.

In conventional stability analyses, the porous medium is typically assumed homogeneous, the perturbation being imposed either externally or as a result of small fluctuations in permeability. In this sense, the problem is similar to the classical Saffman-Taylor¹ problem for displacement in a homogeneous Hele-Shaw cell. As is well known, in the absence of gravity and in the long-wave limit, displacements are stable, if the ratio of the end-point viscosities, $M = \frac{\mu_+}{\mu_-}$, is smaller than one, and they are unstable, otherwise. Here, subscripts + and - refer to the initial (downstream) and injected (upstream) fluids, respectively. Viscous Fingering (VF) emerges as the unstable pattern at conditions of instability.

Heterogeneity will interfere both with the onset and the development of the instability. Most studies have focused on its effect on the fully-developed instability. Based on numerical simulations, Waggoner et al.² classified fully-developed patterns in three regimes, Viscous Fingering, Dispersion and Channeling, depending on the values of M , the variance of the heterogeneity and its correlation length. In this classification VF is the unstable regime when both the variance and the correlation lengths are small. Analogous ideas were expressed in the work of Araktingi and Orr³. In these studies, heterogeneity was modeled as a stationary, spatially correlated random field.

The interplay between heterogeneity and fully-developed viscous instability has also been addressed analytically. Welty and Gelhar⁴ derived evolution equations for miscible displacements (including gravity) based on small-perturbation theory. They showed that a convection-dispersion equation is applicable when displacements are long-wave stable, but that in the unstable case the effective dispersion coefficient diverges with time. Lenormand

and Wang⁵ proposed a model that captures instability and heterogeneity through the additive contributions of two terms, a modified convective term and a dispersive term, the latter following the Gelhar and Axness⁶ passive tracer dispersion.

The effect of heterogeneity on the stability of displacement fronts has been considered in a limited number of studies. Using numerical simulation, Tan and Homsy⁷ inferred that a resonance between the most dominant wavelength of the instability, as determined from the dispersion relation in a homogeneous medium, and heterogeneity will enhance the instability. The idea was revisited several years later by de Wit and Homsy^{8,9}, who provided a stability analysis of miscible displacement including dispersion, in a sinusoidal, periodic permeability field. Using a small amplitude expansion, these authors showed that unstable wavelengths are amplified when they are in resonance with the underlying heterogeneity, the effect being largest at higher values of M and when the heterogeneity is transverse to the direction of displacement, as is the case in a displacement in a layered system, where the layers are parallel to the main flow direction. Essentially the opposite case, where the displacement is in a direction perpendicular to the layers, was studied numerically by Chen and Neuman¹⁰ in the context of immiscible displacement. These authors investigated the linear evolution of instabilities of a wetting front in a randomly stratified medium.

In this paper we consider the latter problem, namely displacements across a stratified system, but in the context of miscible flow. Miscible displacements find applications in various areas such as enhanced oil recovery, channeling in packed columns and in-situ solvent injection techniques for groundwater remediation. The specific question we address is what is the effect of a longitudinal variation in permeability on the stability of miscible displacements. As in Chen and Neuman¹⁰, heterogeneity is assumed only in the direction of displacement, perpendicular to the stratification (Figure 1a). While this is taken to isolate a specific heterogeneity effect, it is not as restrictive as it might appear, since applications under such conditions are not uncommon in natural porous media and soils, many of which are stratified. We follow the asymptotic approach of Hickernell and Yortsos¹¹ to study the stability of perturbations of long and short wavelengths. Although based on the absence of dispersion, this approach can be extended to account for the stabilizing effect of transverse dispersion, using the modification described in Loggia et al¹². Moreover, because the emphasis is on long

wavelengths in the absence of dispersion, the analysis can also be extended to immiscible displacements, in the absence of capillarity, subject to some simple modifications.

We find that longitudinal heterogeneity can affect qualitatively (in addition to quantitatively) the long-wave instability. Displacements are predicted to be more unstable or more stable, as the permeability increases or decreases in the direction of displacement, respectively. One particularly simple such variation is a discontinuity in permeability. While this heterogeneity effect could be argued to be the simple result of the increase (or decrease) in the overall mobility, it is in fact due to an additional contribution, arising from the variation of permeability. The latter is fixed in space, while viscosity, being concentration-dependent, follows the evolving concentration field. In addition, we find the rather surprising result that under certain conditions, displacements predicted to be stable (or unstable), based on end-point stability criteria, such as the Saffman-Taylor, can in fact become unstable (or stable), for sufficiently large permeability contrasts. In the absence of gravity, this change of stability occurs only if the base-state mobility profile is non-monotonic. Otherwise, the effect is only quantitative, there being no change of sign on the rate of growth. In the presence of gravity, this effect exists for monotonic profiles as well. We note that non-monotonic mobility profiles arise in various applications, for example in solvent injection in cases where the dependence of viscosity on the local concentration is non-monotonic¹³, and in immiscible displacement in oil recovery applications, due to the dependence of the total mobility on relative permeabilities¹⁴.

The paper is organized as follows: We first describe the formulation of the problem and obtain the eigenvalue problem in the absence of dispersion. Asymptotic results are derived in the long and short wave limits, which are subsequently verified by the numerical solution of the eigenvalue problem. The effect of non-monotonic viscosity profiles in altering the stability is interpreted using the vorticity of the flow. The effect of gravity is also briefly discussed.

II. FORMULATION

Consider the miscible displacement of fluid 1 by fluid 2 at constant rate q_T , in a layered system of constant porosity ϕ , in a direction x across the stratification, as shown in Fig. 1. The displacement is characterized by the concentration (volume fraction) of the injected fluid, C , which we take to be equal to 1 at injection and 0 initially. Viscosities and densities are functions of C . We follow Hickernell and Yortsos¹¹ and write in the absence of diffusion, dispersion and gravity the governing equations

$$\nabla \cdot \mathbf{q} = 0 \quad (1)$$

$$\mathbf{q} = -\frac{k(x)}{\mu} \nabla P \quad (2)$$

$$\phi \frac{\partial C}{\partial t} + \mathbf{q} \cdot \nabla C = 0 \quad (3)$$

where \mathbf{q} is the flow velocity, P is pressure, $k(x)$ is the permeability of the porous medium, varying in the direction of displacement x and $\mu(C)$ is the fluid viscosity, a function of concentration, to be specified in more detail below. Neglected in the above are dispersion, compressibility and gravity. Effects of density will be considered in a later section. Under the above assumptions, there exists a one-dimensional base-state, the concentration of which satisfies

$$(q_T - \phi v) \frac{dC}{d\xi} = 0 \quad (4)$$

in terms of the moving coordinate $\xi = x - vt$, where

$$v = \frac{q_T}{\phi} \quad (5)$$

In view of (5), equation (4) admits an arbitrary solution for the base-state concentration profile. However, the analysis can be extended to account for dispersion in an approximate fashion, by separately including longitudinal dispersion in the base state, and transverse dispersion in the perturbation, as suggested in Loggia et al.¹². Hence, even though (4) admits

an arbitrary solution, we will assume in the following that the base state concentration has an erfc-type profile (Fig. 1b), and this will be used in the numerical examples. The base state viscosity profile varies according to the specified viscosity-concentration relation. A schematic, indicating possible non-monotonic dependence, is shown in Fig. 1c.

We next introduce appropriate dimensionless variables, denoted by subscript D , and transform the equations in dimensionless moving coordinates to obtain

$$\nabla \cdot \left(\frac{k_D}{\mu_D} \nabla P_D \right) = 0 \quad (6)$$

$$\mathbf{q}_D = - \frac{k_D}{\mu_D} \nabla P_D \quad (7)$$

$$\frac{\partial C_D}{\partial t_D} + (\mathbf{q}_D - \mathbf{i}) \cdot \nabla C_D = 0 \quad (8)$$

where \mathbf{i} is the unit vector in the x direction. Then, we perform a linearized stability analysis by taking small perturbations and normal modes

$$C = \bar{C}(\xi) + C' = \bar{C}(\xi) + c \exp(i\alpha y + \omega t) \quad (9)$$

$$P = \bar{P}(\xi) + P' = \bar{P}(\xi) + \exp(i\alpha y + \omega t) \quad (10)$$

$$\mu = \bar{\mu}(\xi) + \frac{d\bar{\mu}}{dC} C' = \bar{\mu}(\xi) + \frac{d\bar{\mu}}{dC} c \exp(i\alpha y + \omega t) \quad (11)$$

where the base state is denoted by overbar, we have dropped the subscript D for convenience and where α and ω denote the wavenumber and rate of growth of the disturbance. Substitution in the governing equations and linearization leads after several manipulations to the following equation

$$\frac{d}{d\xi} \left[\frac{k}{\bar{\mu} \left(\omega - \frac{d\ln \bar{\mu}}{d\xi} \right) \frac{dp}{d\xi}} \right] - \frac{\alpha^2 kp}{\bar{\mu} \omega} = 0 \quad (12)$$

This can be brought into a more convenient form by introducing the streamfunction perturbation ψ ,

$$\frac{d\psi}{d\xi} = \frac{kp}{\bar{\mu}} \quad (13)$$

Upon substitution in (12) and integration we finally get

$$\frac{d}{d\xi} \left[\frac{\mu}{k} \frac{d\psi}{d\xi} \right] = \frac{\alpha^2}{\omega} \left[\frac{\mu}{k} \omega - \frac{1}{k} \frac{d\mu}{d\xi} \right] \psi \quad (14)$$

where we have also removed the overbar from the base-state. Along with vanishing far-field conditions, this constitutes the eigenvalue problem to be solved. Before we proceed, we make the following remarks:

1. Given that k is a function of the moving coordinate ξ , the tacit assumption was made that the permeability is frozen during the evolution of the perturbation. Freezing of the base-state is a common assumption in stability problems and has frequently been used before, see de Wit and Homsy^{8,9} and Tan and Homsy¹⁵.
2. The effect of permeability does not enter in the eigenvalue problem solely as a total mobility (k/μ) effect. Instead, there is a decoupling of the two mobility contributions (of k and of μ) as shown in the RHS of (14). This reflects the fact that viscosity is only a function of concentration, the perturbation of which is transported by convection (and diffusion), while the permeability heterogeneity is position-dependent only.
3. To include transverse (but not longitudinal) dispersion, which exerts a stabilizing effect, in the eigenvalue problem we can make in (14) the substitution

$$\omega \rightarrow \omega + D_T \alpha^2 \quad (15)$$

where D_T is a normalized transverse dispersion coefficient (see also Loggia et al.¹²). In this approximation, transverse dispersion is linearly added to the solution of the eigenvalue problem (14). On the other hand, incorporating longitudinal dispersion is not as simple, and will raise the order of the eigenvalue problem to four (e.g Tan and Homsy¹⁵, Manickam and Homsy¹³). This will not be considered here.

In the subsequent sections we will provide asymptotic solutions to (14) in the two limits of small and large α , Respectively. These will then be verified by the full numerical solution of the problem.

A. Asymptotic analysis at large wavelengths

We follow an analysis similar to Hickernell and Yortsos¹¹ and consider the limit

$$\sigma = \alpha^2/\omega \rightarrow 0 \quad (16)$$

Taking the expansion

$$\alpha = \alpha_1 \sigma + \alpha_2 \sigma^2 + \dots \quad (17)$$

we have

$$\omega = \alpha_1 \alpha + \frac{\alpha_2}{\alpha_1} \alpha^2 + \dots \quad (18)$$

This limit is singular, thus we must consider an inner region, $|\xi| \ll \alpha^{-1}$, and two outer regions, $|\xi| \gg \ln \omega$. The solution in the inner region is denoted by $\tilde{\psi}$ and in the outer by $\hat{\psi}^{(s)}$, where s is the sign variable (\pm). We then expand the variables in terms of powers of σ

$$\tilde{\psi} = \tilde{\psi}_0 + \sigma \tilde{\psi}_1 + \sigma^2 \tilde{\psi}_2 + \dots \quad (19)$$

$$\hat{\psi}^{(s)} = \hat{\psi}_0^{(s)} + \sigma \hat{\psi}_1^{(s)} + \sigma^2 \hat{\psi}_2^{(s)} + \dots \quad (20)$$

Under the assumption that the permeability approaches constant far-field values, k_s , which will be assumed here, the outer solutions are exponential functions

$$\hat{\psi}_j^{(s)} = \hat{\psi}_{j\infty}^{(s)} \exp(-s\alpha\xi) \quad (21)$$

The inner expansion has a leading-order solution which is constant,

$$\tilde{\psi}_0 = 1 \quad (22)$$

and a first-order solution which reads, after one integration,

$$\frac{\mu}{k} \frac{d\tilde{\psi}_1}{d\xi} = -\frac{\mu}{k} + \int_0^\xi \mu \frac{dk^{-1}}{d\xi} d\xi + K_1 \quad (23)$$

Expanding (21) and matching with (22) and (23) allows the determination of α_1 (and K_1). The result reads

$$\alpha_1 = \frac{m_+ - m_- + \int_{-\infty}^{\infty} \frac{\mu}{k^2} \frac{dk}{d\xi} d\xi}{m_+ + m_-} \quad (24)$$

where we introduced the far-field inverse mobilities $m_s = \frac{\mu_s}{k_s}$, and

$$K_1 = \frac{(\alpha_1 + 1)\mu_-}{k_-} + \int_{-\infty}^0 \mu \frac{dk^{-1}}{d\xi} d\xi \quad (25)$$

Equation (24) can also be re-written as

$$\alpha_1 = \frac{\int_{-\infty}^{\infty} \frac{1}{k} \frac{d\mu}{d\xi} d\xi}{m_+ + m_-} \quad (26)$$

We remark the following:

1. In the case of a homogeneous medium, Equation (24) reduces to the well-known Saffman-Taylor result

$$\alpha_1 = \frac{m_+ - m_-}{m_+ + m_-} = \frac{\mu_+ - \mu_-}{\mu_+ + \mu_-} = \frac{M - 1}{M + 1} \quad (27)$$

as expected.

2. At this long-wave limit, the effect of heterogeneity is due to the term $\int_{-\infty}^{\infty} \frac{\mu}{k^2} \frac{dk}{d\xi} d\xi$. As shown in (24) and (26), this is not merely a total mobility effect. Compared to the end-point total mobility values, instability is enhanced if permeability increases in the direction of displacement, and weakened in the opposite case. In addition, equation (26) shows that this effect remains only quantitative, in that it does not affect the sign of α_1 , if the base-state viscosity profile is monotonic, in which case the derivative of viscosity has a constant sign.

3. However, the heterogeneity effect can be non-trivial when the base-case viscosity is *non-monotonic*, in which case, an appropriate form of heterogeneity may lead to a change in the sign of α_1 , opposite to what is predicted based on the end-point difference, equation (27).

4. In the absence of dispersion, the eigenvalue problem admits an infinite family of eigenvalues¹¹, one of which scales with α in the long-wave limit, all others scaling with α^2 . In the presence of dispersion, the latter become sub-dominant.

A simple example demonstrating the heterogeneity effect is displacement with variable mobility across a discontinuity in permeability at $\xi = 0$, where the expression for α_1 becomes

$$\alpha_1 = \frac{m_+ - m_- + \mu_0 \left(\frac{1}{k_-} - \frac{1}{k_+} \right)}{m_+ + m_-} \quad (28)$$

and where we defined $\mu_0 = \mu(\xi = 0)$. Equation (28) shows that for a fixed end-point mobility contrast $\frac{m_+ - m_-}{m_+ + m_-}$, the effect of the discontinuity is to favor destabilization, if the permeability increases in the direction of displacement, and stabilization in the opposite case. For an end-point unstable displacement, $m_+ > m_-$, the displacement will actually be stabilized if the permeability decrease in the direction of displacement is sufficiently large, such that

$$\frac{k_- - k_+}{k_- k_+} > \frac{m_+ - m_-}{\mu_0} \quad (29)$$

Conversely, for an end-point stable displacement, $m_- > m_+$, and a similar non-monotonic profile, the displacement will be destabilized if the permeability increases in the direction of displacement, such that

$$\frac{k_+ - k_-}{k_- k_+} > \frac{m_- - m_+}{\mu_0} \quad (30)$$

Numerical results will be shown below.

Before we proceed, we may note that we can likewise obtain an expression for the second-order term. We find the final result

$$\alpha_2 = -\frac{(I + 2m_+)(I - 2m_-)}{(m_+ + m_-)^3} \int_{-\infty}^{\infty} \frac{kH}{\mu} d\xi \quad (31)$$

where

$$H = \left[\frac{\mu}{k} + \frac{m_-(I + 2m_+)}{I - 2m_-} - \frac{m_+ + m_-}{I - 2m_-} \int_{-\infty}^{\xi} \frac{\mu}{k^2} \frac{dk}{d\xi} d\xi \right] \left[\frac{\mu}{k} - m_- + \frac{m_+ + m_-}{I + 2m_+} \int_{-\infty}^{\xi} \frac{\mu}{k^2} \frac{dk}{d\xi} d\xi \right] \quad (32)$$

and where we defined $I = \int_{-\infty}^{\infty} \frac{\mu}{k^2} \frac{dk}{d\xi} d\xi$. An analysis of the effect of the various parameters on α_2 is not as easy, due to its complex dependence. To complete the asymptotic description, we will comment on the short-wave limit.

B. Asymptotic analysis at small wavelengths

By proceeding as in Ref. [11], We can readily show that in the limit of small wavelengths and in the absence of dispersion, the largest eigenvalue for the rate of growth ω_{max} in (14) is the maximum in the logarithmic derivative of the viscosity profile,

$$\omega_{max} = \max_{\xi} \left[\frac{d \ln \mu}{d \xi} \right] \quad (33)$$

This expression does not depend on the heterogeneity of the medium. As in the homogeneous case, it suggests instability if the base state has a segment of increasing viscosity. Of course, transverse dispersion, which at large α scales as $-D_T \alpha^2$ (compare with (15)), will dominate over (33). Thus, in the presence of dispersion, the most dominant wavelength is approximately the one corresponding to the maximum of $\omega(\alpha) - D_T \alpha^2$, where $\omega(\alpha)$ is the solution of the dispersionless eigenvalue problem (14). It follows that the effect of a longitudinal heterogeneity in permeability on the stability of a displacement in a stratified medium is pronounced at long waves.

III. NUMERICAL RESULTS

To verify the analytical predictions, the eigenvalue problem (14) was solved numerically using the shooting method described in Chikhliwala et al¹⁴. For convenience, we considered a dispersion-like base-state concentration profile

$$C = \frac{1}{2} \operatorname{erfc}(\xi) \quad (34)$$

and the non-monotonic model of Manickam and Homsky¹³, containing two parameters, the ratio in end-point viscosities, M , and the normalized maximum (or minimum) viscosity, M_0 , here taken at $\xi = 0$. To model a monotonic change in permeability we take the model

$$k = 1 + a \operatorname{tanh} \left(\frac{\xi}{b} \right) \quad ; \quad -1 < a < 1 \quad (35)$$

where $a > 0$, or $a < 0$, indicates a permeability increase, or decrease, respectively, and b scales the region over which a permeability change occurs.

Consider, first, the predictions from the asymptotic analysis. Figs. 2-3 show the variation of α_1 as a function of a for the case $b = 1$ and for two different base-state viscosity profiles, one corresponding to a nominally stable displacement for a homogeneous system ($M = 0.2 < 1$, Fig. 2), and another to an unstable displacement for a homogeneous system ($M = 5 > 1$, Fig. 3). The corresponding base-state profiles are also shown in the respective figures. Note that the large intermediate viscosity values in these examples were only taken for convenience and are not indicative of any strong restriction on viscosity, in order to result in the behavior shown. As predicted, heterogeneity can alter the results obtained based on the end-point mobilities: For the stable end-point case ($M = 0.2$), the displacement becomes unstable if the heterogeneity contrast exceeds a critical value of approximately $a = 0.28$. For the unstable end-point case ($M = 5$), the displacement is stabilized if a is smaller than a value approximately equal to $a = -0.4$. The expression derived for α_2 was also computed, but a clear trend did not emerge. It was decided, instead, to consider the effect of a on the overall dispersion relation, for which the numerical solution of the eigenvalue problem was used.

Fig. 4 shows the dispersion relation $\omega(\alpha)$ for the case $M = 0.2$ and $a = 0.5$ (permeability contrast of 3:1), for which the conventional theory for a homogeneous system predicts stability ($\alpha_1 = -0.61$), but the asymptotic theory for a heterogeneous system predicts instability ($\alpha_1 = 0.3366$). We see that the theory is in good agreement with the numerical solution. At small α , the behavior is linear, with a slope close to the predicted. As α increases, ω deviates from the linear behavior and at large α it asymptotes the limiting value (33), which for this particular example is predicted to be 0.9671. The behavior is similar to that for the homogeneous case, in that the long-wave region is controlled by α_1 , and the short-wave by ω_{max} . Fig. 5 shows the dispersion relation $\omega(\alpha)$ for the case $M = 5$ and $a = -0.7$ (permeability contrast of 3:17), for which the conventional theory for a homogeneous system predicts instability ($\alpha_1 = 0.66$), but the present long-wave theory predicts stability ($\alpha_1 = -0.1613$). The curve shown in Fig. 5 satisfies well the theoretical predictions. We have also studied numerically the stability of various other forms of longitudinal heterogeneity, including sinusoidal and random perturbations. The results obtained were consistent with the analysis. Multiple changes in permeability (for example a two-step variation) will tend to enhance the effect considered, if both steps are in the same direction, but to diminish it otherwise.

Thus, it is apparent that longitudinal heterogeneity can substantially alter the stability of displacements. This, provided that the regions of heterogeneity and mobility changes coincide (compare with (24) or (26)). For a flat viscosity profile, heterogeneity will have no effect, as anticipated. Thus, in a transient displacement in a medium with a permeability discontinuity, the effect of heterogeneity will start becoming important as the advancing profile approaches and interferes with the place of discontinuity.

IV. A MECHANISTIC INTERPERTATION

For an interpretation of the heterogeneity effect we consider the vorticity of the flow

$$\Omega = \nabla \mathbf{x} \mathbf{q} \quad (36)$$

In the small fluctuation limit of the linear analysis, we can use the expansions described in section II to find for the z -component

$$\Omega_z = \frac{d \ln \mu}{d C} \frac{\partial C'}{\partial y} - v' \frac{\partial \ln \left(\frac{\mu}{k} \right)}{\partial x} \quad (37)$$

where v' is the y -component of the velocity field after the perturbation was imposed. Equivalently, we may rewrite (37) as

$$\Omega_z = \frac{\partial \ln \left(\frac{\mu}{k} \right)}{\partial x} \left(\frac{\partial c'}{\partial y} - v' \right) + \frac{\partial \ln k}{\partial x} \frac{\partial c'}{\partial y} \quad (38)$$

where we defined $c' = \frac{C'}{\frac{\partial C}{\partial x}}$. Either of these equations shows that vorticity is generated by separate contributions from the effective mobility and the permeability (or the viscosity). For example, the last equation shows that if the effective viscosity increases in the direction of displacement, which favors instability, then a concomitant increase in k further destabilizes the flow, while a decrease in k acts to stabilize it. Likewise, if the effective viscosity decreases in the direction of displacement, which favors stability, an increase in k will destabilize the flow, while a decrease will further enhance stability.

The above explains why a permeability increase or decrease enhances or diminishes the instability, but does not show the possible reversal of stability in the case of a non-monotonic profile. To interpret the latter, consider the vortices formed at large wavelengths. As found

above, it is in this limit, where the effect of longitudinal heterogeneity is strongest, and where we can benefit from the asymptotic analysis. At large wavelengths, there is a single row of (either stabilizing or destabilizing) vortices formed. The center of each vortex is the place where the streamfunction is maximum, which from (23) is the place ξ^* where the following applies

$$-\frac{\mu^*}{k^*} + \int_0^{\xi^*} \mu \frac{dk^{-1}}{d\xi} d\xi + \frac{(\alpha_1 + 1)\mu_-}{k_-} + \int_{-\infty}^0 \mu \frac{dk^{-1}}{d\xi} d\xi = 0 \quad (39)$$

To understand the effect of heterogeneity in a non-monotonic viscosity profile, consider, first, a homogeneous displacement. Then, use of (25) in (39) leads to

$$\mu^* = \frac{2\mu_- - \mu_+}{\mu_- + \mu_+} = \frac{2M}{M + 1} \quad (40)$$

namely the vortex center is at the place where the viscosity is the harmonic average of the end point viscosities, or, equivalently, where the mobility is the arithmetic average of the end-point mobilities. This result for the homogeneous problem is independent of whether or not the profile is non-monotonic. Consider, next, a heterogeneous field, which for the sake of simplicity we take to be a discontinuity at $\xi = 0$. As a result of the imposed heterogeneity, the vortex center will shift. By a simple manipulation of (39) it can be shown that the new position is determined from the following:

If $\xi^* < 0$, then ξ^* is the place where the normalized viscosity has the value

$$M^* = \frac{2(M - a(M - M_0))}{M + 1 - a(M - 1)} \quad (41)$$

where we defined $M^* = \frac{\mu^*}{\mu_-}$ and $M_0 = \frac{\mu_0}{\mu_-}$. If $\xi^* > 0$, then it is where

$$M^* = \frac{2M(1 + a - M_0a)}{M + 1 - a(M - 1)} \quad (42)$$

Here, As a varies, the vortex center, hence the corresponding value M^* , moves along the base-state profile, in a direction determined from the two parameters M and M_0 . Interestingly, the different branches of the non-monotonic profile (where there exists multiplicity of viscosity, for example the regions $\xi < 0$ and $\xi > 0$ in the profiles of Fig. 1) are reached by opposite permeability contrasts. Indeed, M_0 is the limit of both (41) and (42), however it is reached

from the left ($\xi \rightarrow 0-$, equation (41)) when $a \rightarrow 1$, and from the right ($\xi \rightarrow 0+$, equation (42)) when $a \rightarrow -1$.

To be more specific, consider non-monotonic profiles and take first, the case of an end-point stable displacement, where $M < 1$, but $M_0 > 1 > M$ (Fig. 6a). In the homogeneous case ($a = 0$), M^* is the harmonic average of 1 and M , and consequently the vortex center is located somewhere in $\xi > 0$ (point I in Fig. 6a), which is a region with a decreasing viscosity in the direction of displacement. As a decreases (becoming negative), the vortex center shifts in the direction of increasing μ (see equation (42)), which here is the direction of decreasing ξ (points I to O in Fig. 6a). However, we can show that it always stays in the branch corresponding to $\xi > 0$, which has a decreasing viscosity in the direction of displacement. Indeed, equation (42) shows that $M^* \leq M_0$ as a decreases, the equality being reached in the limit $a \rightarrow -1$ (where $k_+ \rightarrow 0$, and the displacement is most stable). Because it stays in a region of decreasing mobility, the displacement remains stable (see also below). On the other hand, when a increases to positive values, the vortex center shifts in the opposite direction, of decreasing μ , which is now the direction of increasing ξ (points I to ∞ , denoted as P_∞ in Fig. 6a). Larger values of a result in the vortex moving further to the right. If instability conditions do not hold, namely if the profile is monotonic and $M_0 < 1$, the vortex center will reach a limiting point (for example, point P in Fig. 6a) where $M^* = M(2 - M_0)$, and the displacement remains stable. Note that in Fig. 6a we have assumed that $M_0 > \frac{2M}{M+1}$. However, if the profile is non-monotonic, the vortex moves further and further away, as a increases, and at the limiting value

$$a_\infty = \frac{1 - M}{2M_0 - M - 1} \quad (43)$$

it approaches ∞ . This moving away from the region where mobility changes occur, weakens the stabilizing influence of the profile and at the limiting point the displacement is neutrally stable. As can be shown by a direct comparison with (28)-(30), this is the point where heterogeneity qualitatively affects the stability for the first time ($\alpha_1 = 0$) and renders the displacement unstable. From this point on, further increases in a can only be accommodated if the vortex center jumps to the other branch of the profile (namely at $-\infty$, denoted in the figure as M_∞), from where now an increase in a shifts the vortex center in the direction of

increasing ξ , namely from M_∞ to O (Fig. 6a). Since now the vortex resides in the region where the viscosity increases with position, the displacement is unstable.

A similar interpretation holds for the other case, where the displacement is end-point unstable ($M > 1$ with $M_0 > M > 1$, Fig. 6b). In the homogeneous case ($a = 0$), the vortex is located somewhere in $\xi < 0$ (point I in Fig. 6b). As a increases, the vortex center shifts in the direction of increasing μ , which here is the direction of increasing ξ (points I to O in Fig. 6b). As in the analogous case above, the vortex always stays in the branch with $\xi < 0$, namely that with increasing viscosity, the value M_0 being approached in the limit $a \rightarrow 1$ (where $k_- \rightarrow 0$). Because the vortex lies in a region of increasing mobility, the displacement remains unstable. However, when a decreases to negative values, the vortex shifts in the opposite direction, of decreasing μ , which is now the direction of decreasing ξ (points I to M_∞ in Fig. 6b). If the profile is monotonic, $M_0 < M$, the vortex center will reach a limiting point M^* , where $M^* = 2 - \frac{M_0}{M}$, and the system remains unstable. However, if the profile is non-monotonic, the vortex moves further and further away, as a decreases, and at the limiting value a_∞ , it approaches M_∞ . Again, this moving away from the region where mobility changes occur, weakens the destabilizing influence of the profile and at the limiting point the displacement is neutrally stable. From this point on, further decreases in a can be accommodated only if the vortex center jumps to the other branch of the profile, where now a decrease in a makes the vortex center to move in the direction from P_∞ to O (Fig. 6b). Since the vortex resides in the region where the viscosity decreases in the direction of displacement, the displacement is now stable.

A few additional remarks are needed to strengthen the above arguments. First, we need to show that vortices in a region of decreasing viscosity profiles are stabilizing, and vice versa. For this we borrow arguments similar to Manickam and Homsy¹³ (although in this long wavelength limit, there is only one row of vortices in contrast to the pair of rows considered in the short wave analysis in Ref. [13]). In the region of decreasing viscosity in the direction of displacement, any two adjacent counter-rotating vortices bring low viscosity fluid from the downstream to the upstream direction and high viscosity fluid from the upstream to the downstream direction as indicated in Fig. 7a. The first action lowers the resistance to flow in a direction that opposes the instability, while the second increases the resistance to

flow in a direction that enhances the instability. Both, therefore, act to stabilize the flow. Conversely, in the region of increasing viscosity in the direction of displacement, two adjacent vortices will bring high viscosity fluid from the downstream to the upstream direction and low viscosity fluid from the upstream to the downstream direction in the directions indicated in Fig. 7b. The effect is opposite to the previous, with the resistance to flow decreasing in the direction that enhances the instability and increasing in the direction that stabilizes the flow. The overall effect is to further destabilize the flow.

To demonstrate the previous analysis we plot the center of a single vortex, obtained from the numerical solution of the eigenvalue problem for a fixed value of the wavenumber ($\alpha = 0.001$) and for two different cases. Fig. 8 shows three snapshots corresponding to the end-point stable profile of Fig. 6a (where $M = 0.2$ and $M_0 = 3$) and for three different values $a = 0, -0.5$ and 0.5 . Here, $a_\infty = 0.1667$, thus the second case corresponds to a stable displacement (where $\xi > 0$), while the last case to an unstable displacement. It is clear from Fig. 8 that the vortex shifts to the left as a decreases and that for $a > a_\infty$ it jumps to the destabilizing branch $\xi < 0$. Conversely, the case corresponding to an end-point unstable profile is shown in Fig. 9 (where $M = 5$ and $M_0 = 10$) for $a = 0, -0.5$ and 0.5 . The first two values correspond to unstable displacement, the last to a stabilized displacement. It is clear that the vortex stays in the unstable branch for the first two cases, moving in the direction predicted from the above, while in the latter case where a decreases below the limiting value $a_\infty = -0.2857$, it jumps to the stabilizing branch.

V. EFFECT OF GRAVITY

The above analysis can be readily extended to account for effects of gravity, when the density is allowed to vary with concentration. We consider the case in which gravity acts only in the direction of displacement, as for example, in 2-D inclined systems, where the transverse direction, $-y$, is the horizontal. The analysis also covers the important case of a vertically stratified system, where the displacement occurs in the vertical direction.

When density is a function of concentration, the governing mass and momentum equations become

$$\frac{\partial \rho}{\partial t} + \nabla \cdot (\rho \mathbf{q}) = 0 \quad (44)$$

$$\mathbf{q} = -\frac{k}{\eta}(\nabla P - \rho \mathbf{g}), \quad (45)$$

where \mathbf{g} is the acceleration of gravity and ρ the density of fluid. We proceed as before following closely Ref. [11]. After considerable manipulations, the following eigenvalue problem is obtained

$$\frac{d}{d\xi} \left[\frac{\mu}{k} \frac{d\psi}{d\xi} \right] = \frac{\alpha^2}{\omega} \left[\frac{\mu}{k} \omega - \frac{1}{k} \frac{d\mu}{d\xi} + G \frac{d\rho}{d\xi} \right] \psi \quad (46)$$

where all variables are dimensionless, the density is normalized with a reference density ρ_0 , and we have defined the gravity number $G = \frac{k_0 \rho_0 g_x}{q_T \mu_-}$. We will consider the solution of (46) in the two asymptotic limits of small and large α .

In the limit of small α , the leading coefficient α_1 is found to be

$$\alpha_1 = \frac{m_+ - m_- - G(\rho_+ - \rho_-) + \int_{-\infty}^{\infty} \frac{\mu}{k^2} \frac{dk}{d\xi} d\xi}{m_+ + m_-} \quad (47)$$

where $(\rho_+ - \rho_-)$ is the normalized density difference of the initial to the injected fluid. We note that heterogeneity can have an important effect on the onset of instability. However, unlike the previous case, a qualitative effect resulting in the change of the sign of α_1 does not necessarily require a non-monotonic viscosity profile. This can be seen by rewriting (47) as

$$\alpha_1 = \frac{\int_{-\infty}^{\infty} \left[\frac{1}{k} \frac{d\mu}{d\xi} - G \frac{d\rho}{d\xi} \right] d\xi}{m_+ + m_-} \quad (48)$$

Comparison with (26) shows that it is the variable $\mu - G \int k d\rho$ that plays the role of an effective viscosity, and which, therefore, can become a non-monotonic profile by a suitable choice of G , k or ρ . The similarity between non-monotonic mobility profiles and gravity driven displacements was exploited earlier for the homogeneous case by Manickam and Homsy¹⁶. For completeness, we also give the asymptotic result for the short wave limit. Then, we find

$$\omega_{max} = \max_{\xi} \left[\frac{d \ln \mu}{d\xi} - G \frac{k}{\mu} \frac{d\rho}{d\xi} \right] \quad (49)$$

In the presence of gravity, heterogeneity also affects the short-wave rates of growth. However, in view of the dominant effect of dispersion in that limit, we elect to not consider it any further.

We demonstrate the longitudinal heterogeneity effect by considering a step change in permeability at $\xi = 0$, in which case (47) reads

$$\alpha_1 = \frac{\left(\frac{\mu_0 - \mu_-}{k_-} - \frac{\mu_0 - \mu_+}{k_+} - N\right)}{m_+ + m_-} \quad (50)$$

where we introduced $N = G(\rho_+ - \rho_-)$. For simplicity, we will consider an exponential viscosity dependence on concentration, which allows us to make the identification $\mu_- = 1$, $\mu_+ = M$ and $\mu_0 = M^{1/2}$ (recall that $C(\xi = 0) = 1/2$). From (50) we obtain

$$\alpha_1 \sim a^2 N - a(M + 1 - 2\sqrt{M}) + M - 1 - N \quad (51)$$

which will be used to study the effect of the heterogeneity parameter a on the shift of the onset of instability. For simplicity, we will assume that conditions of neutrally stable displacement for a homogeneous case apply, namely that $M - 1 = N$. Then, by eliminating N from (51) we find

$$\alpha_1 \sim a(\sqrt{M} - 1)[a(\sqrt{M} + 1) - (\sqrt{M} - 1)] = (M - 1)a(a - a^*) \quad (52)$$

where $a^* = \frac{\sqrt{M}-1}{\sqrt{M}+1}$. Equation (52) has a different behavior depending on the value of M . For $M > 1$ (in which case $N > 0$ at neutral stability for the homogeneous case), α_1 is positive in the intervals $-1 < a < 0$ and $a^* < a < 1$, and negative in the interval $0 < a < a^*$ (Fig. 11a). For $M < 1$ (in which case $N < 0$), α_1 is positive in the interval $a^* < a < 0$, and negative otherwise ($0 < a < 1$ and $-1 < a < a^*$) (Fig. 11b). Thus, a jump in permeability can promote or suppress the onset of instability, depending on the specific conditions. This can be physically translated as follows:

In the case when a less viscous and lighter fluid is displacing downwards a more viscous and heavier fluid (or a heavier fluid is displacing upwards a lighter fluid, $N > 0$) gravity is stabilizing. An increase in permeability in the direction of displacement will further stabilize the displacement, provided that the permeability ratio does not exceed the value \sqrt{M} (for

the present case of an exponential viscosity-concentration dependence). If it does and/or in the case of a permeability decrease in the direction of displacement, the displacement will be destabilized.

Conversely, in the case when a more viscous but heavier fluid is displacing downwards a less viscous but lighter fluid (or a lighter fluid is displacing upwards a heavier fluid, $N < 0$) gravity is destabilizing. A decrease in permeability in the direction of displacement will further destabilize the displacement, as long as the permeability ratio is larger than \sqrt{M} (again for the exponential viscosity-concentration dependence). If it is not and/or in the case of a permeability increase in the direction of displacement, the displacement will be stabilized.

VI. CONCLUSIONS

In this paper, we considered the linear stability of displacements in stratified porous media, where the displacement is perpendicular to the direction of displacement. We used an asymptotic analysis to derive short and long wavelength expansions for the growth rate of disturbances. The heterogeneity has an anticipated long-wave effect, in that it enhances or reduces the instability, depending on whether permeability increases or decreases in the direction of displacement, respectively. However, this effect can be non-trivial, when the viscosity depends in a non-monotonic way on concentration. In this case, the Saffman-Taylor criterion fails to predict the onset of instability which is now additionally dependent on the permeability contrast.

For a fluid with a non-monotonic viscosity profile, a sufficiently high permeability increase in the direction of displacement can render the flow unstable, even though the end point viscosity ratio is smaller than one. Conversely, nominally unstable displacements can be stabilized if the permeability decrease in the direction of displacement is sufficiently large. This behavior is possible if the viscosity profile is non-monotonic, in the absence of gravity, or for arbitrary viscosity profiles when gravity is important. The results were interpreted by noting that contributions to vorticity arise not only from variations in the effective mobility, but also and separately, from variations in permeability, which remains frozen in space.

ACKNOWLEDGEMENTS

This research was partially supported by Contract DE-26AC-99BC15211 of the Department of Energy. The first author (MS) was also partly supported by a Doctoral Fellowship from the National Science Foundation to the USC Environmental Sciences, Policy and Engineering Sustainable Cities Program. These sources of support are gratefully acknowledged.

¹P.G. Saffman and G.I. Taylor, "The penetration of a fluid into a porous medium or Hele-Shaw cell containing a more viscous liquid," Proc. R. London, Ser. A.**245**, 312 (1958).

² J.R. Waggoner, J.L. Castillo and L.W. Lake, "Simulation of EOR processes in stochastically generated permeable media," SPEFE, 173 (1992).

³U.G. Araktingi and F.M. Orr, Jr., "Viscous fingering in heterogeneous porous media," SPE Advanced Technology Series, 71 (1993).

⁴C. Welty and L.W. Gelhar, "Stochastic analysis of the effects of fluid density and viscosity variability on macrodispersion in heterogeneous porous media," Water Resources Res. **27**, 2051 (1991).

⁵R. Lenormand and B. Wang, "A stream-tube model for miscible flow", Transport in Porous Media **18**, 263 (1995).

⁶L.W. Gelhar and C.L. Axness, "Three-dimensional stochastic analysis of macrodispersion in aquifers," Water Resources Res. **19**, 161 (1983).

⁷C.T. Tan and G.M. Homsy, "Simulation of nonlinear viscous fingering in miscible displacement," Phys. Fluids **31**, 1330 (1988).

⁸A. DeWit and G.M. Homsy, "Viscous Fingering in periodically heterogeneous porous media. I. Formulation and linear instability," J. Chem. Phys. **107**, 22 (1997).

⁹A. DeWit and G.M. Homsy, "Viscous Fingering in periodically heterogeneous porous media. II. Numerical simulations," J. Chem. Phys. **107**, 9619 (1997).

¹⁰G. Chen and S.P. Neuman "Wetting front instability in randomly stratified soils," Phys. Fluids **8**, 353 (1996).

¹¹F.J. Hickernell and Y.C. Yortsos, "Linear stability of miscible displacement processes in porous media in the absence of dispersion," Stud. Appl. Math. **74**, 93 (1986).

¹²D. Loggia, D. Salin and Y.C. Yortsos, "The effect of dispersion on the stability of non-

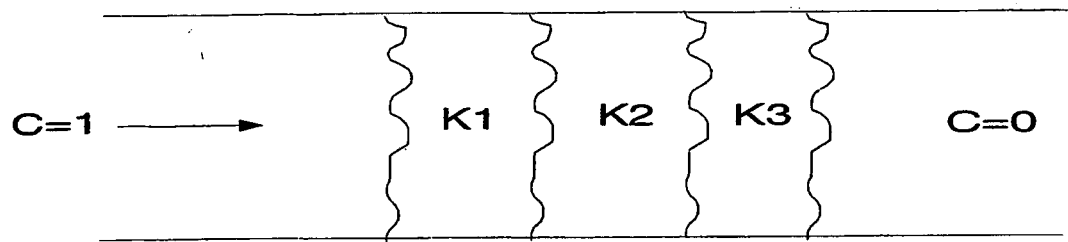
monotonic mobility profiles in porous media," *Phys. Fluids* **10**, 747 (1998).

¹³O. Manickam, O. and G.M. Homsy, "Stability of miscible displacements in porous media with non-monotonic viscosity profiles," *Phys. Fluids* **A.5**, 1356 (1993).

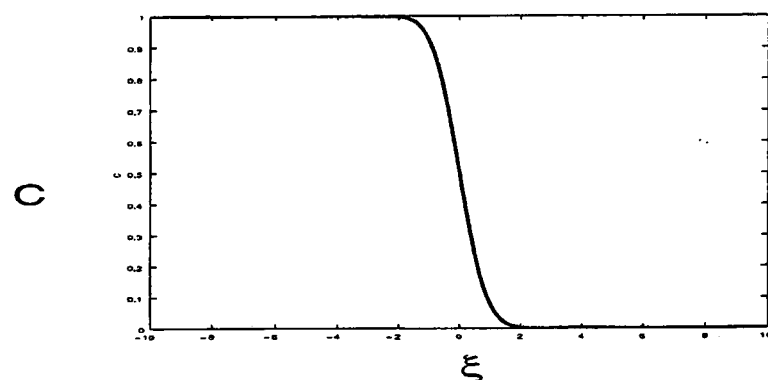
¹⁴E.D. Chikhliwala, A.B. Huang and Y.C. Yortsos, "Numerical study of the linear stability of immiscible displacement in porous media," *Transport in Porous Media* **3**, 257 (1988).

¹⁵C.T. Tan and G.M. Homsy, "Stability of miscible displacements in porous media: Rectilinear flow," *Phys. Fluids* **29**, 3549 (1986).

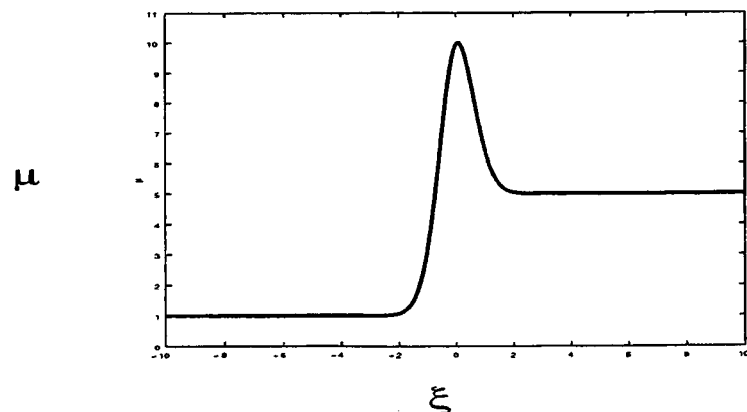
¹⁶O. Manickam and G.M. Homsy, "Fingering instabilities in vertical miscible displacement flows in porous media," *J. Fluid Mech.* **288**, 75 (1995).



(a)



(b)



(c)

Figure 1: Schematic of the process considered: (a) Displacement in a stratified medium, (b) base state concentration profile, (c) corresponding non-monotonic viscosity profile.

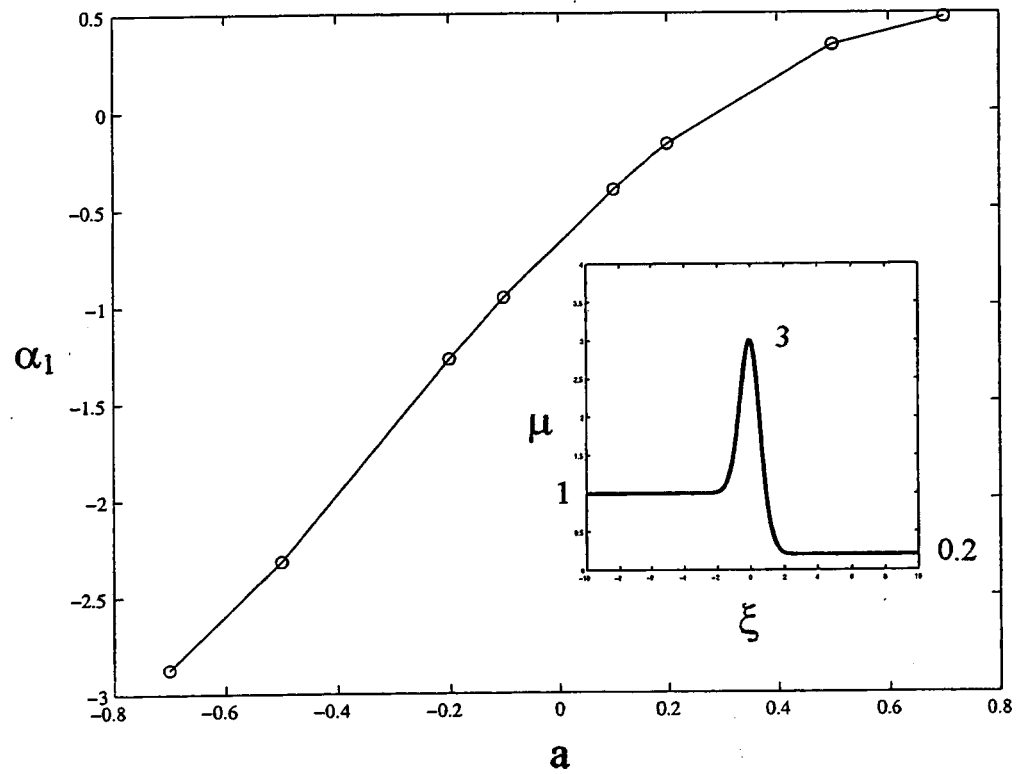


Figure 2: Effect of permeability contrast on the long-wave rate of growth for a non-monotonic profile with stable end-point mobility contrast ($M = 0.2$, $\mu_0 = 3$).

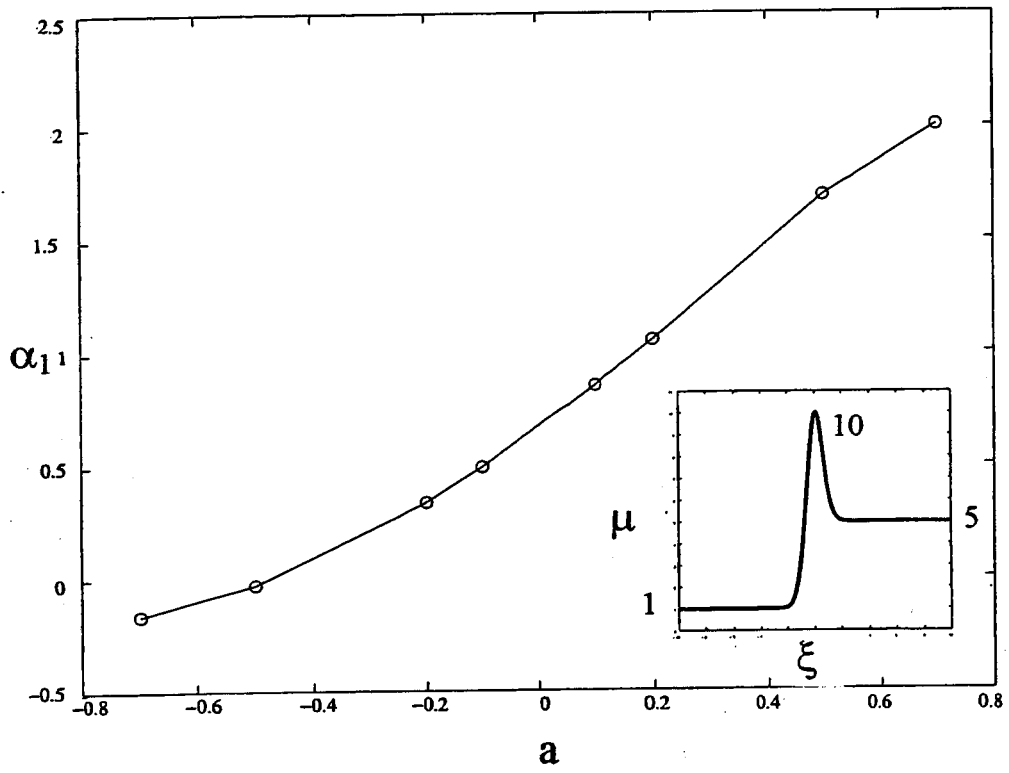


Figure 3: Effect of permeability contrast on the long-wave rate of growth for a non-monotonic profile with stable end-point mobility contrast ($M = 5$, $\mu_0 = 10$).

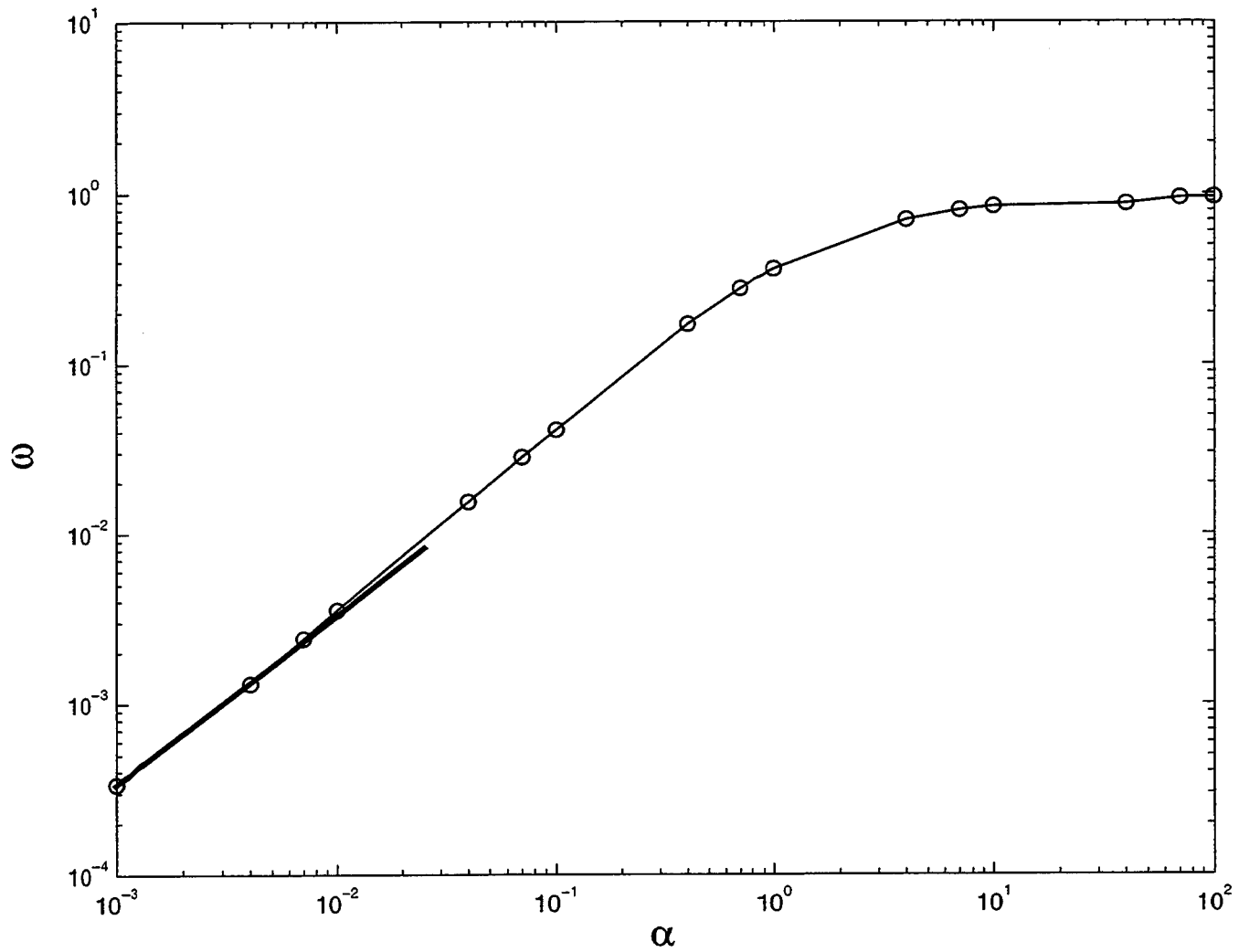


Figure 4: Dispersion relation for $M = 0.2$ and $M_0 = 3$. The heavy solid line is the analytical prediction.

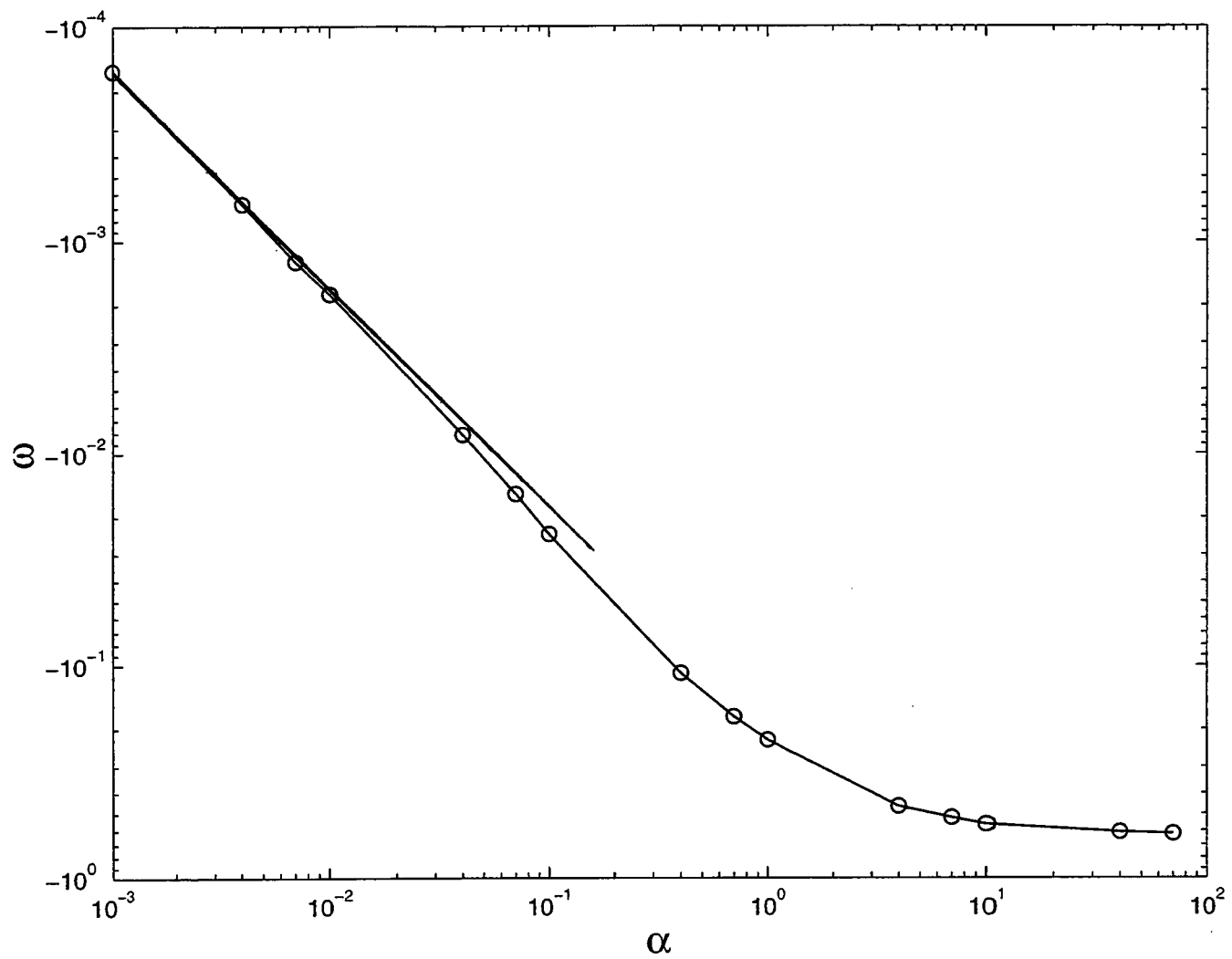


Figure 5: Dispersion relation for $M = 5$ and $M_0 = 10$. The heavy solid line is the analytical prediction.

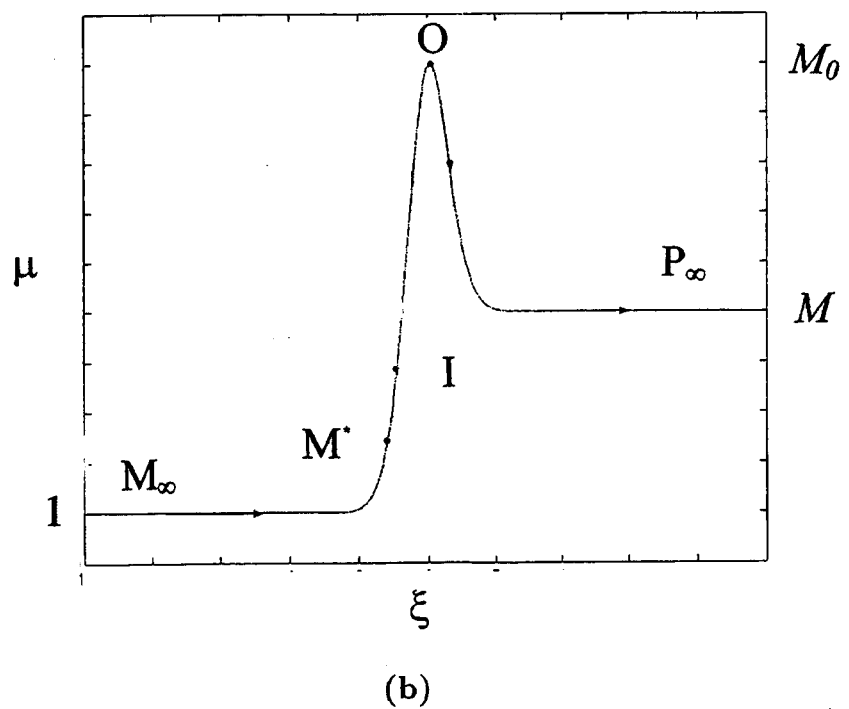
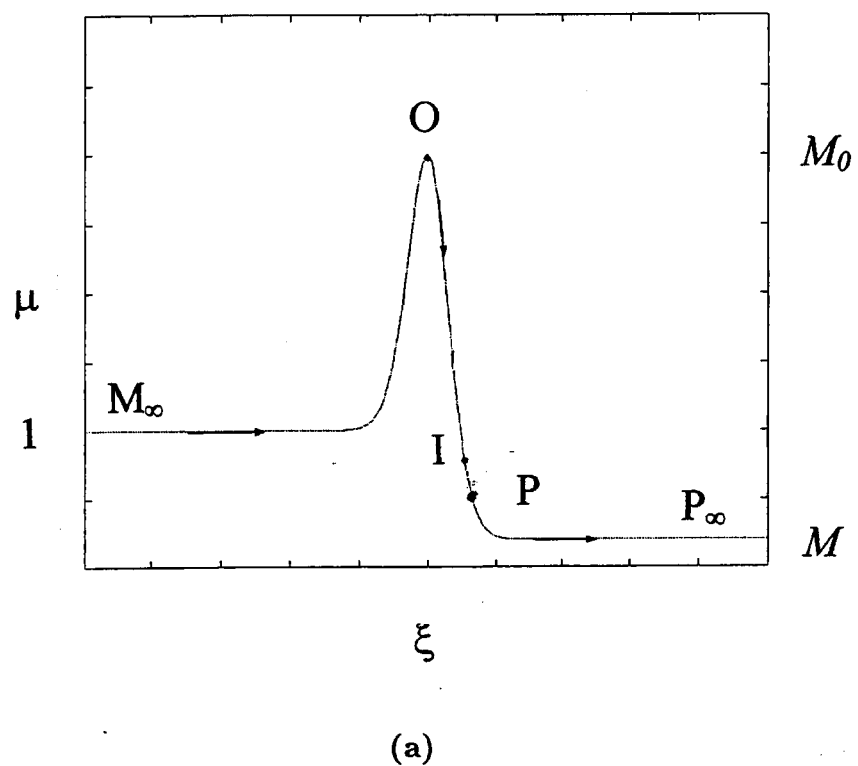


Figure 6: Location of the vortex as a function of the permeability contrast: (a) End-point stable displacement, (b) end-point unstable displacement. Arrows indicate the direction of increasing a .

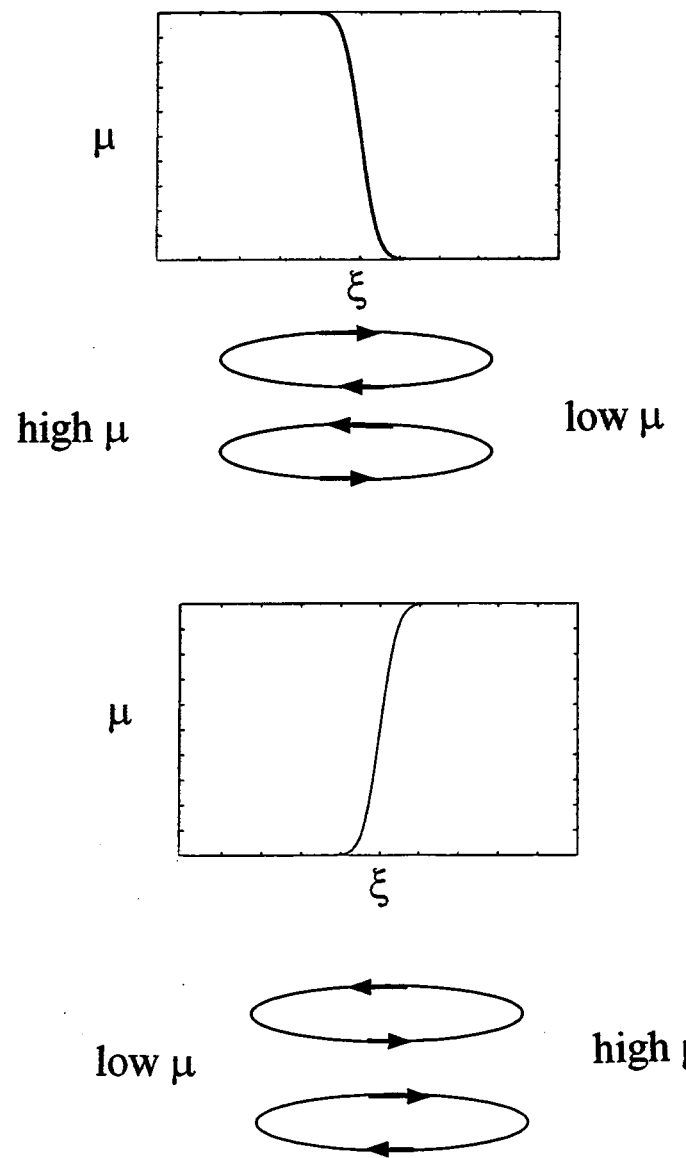


Figure 7: Mechanistic interpretation of stabilization/destabilization mechanisms for the cases of: (a) Decreasing viscosity, (b) increasing viscosity.

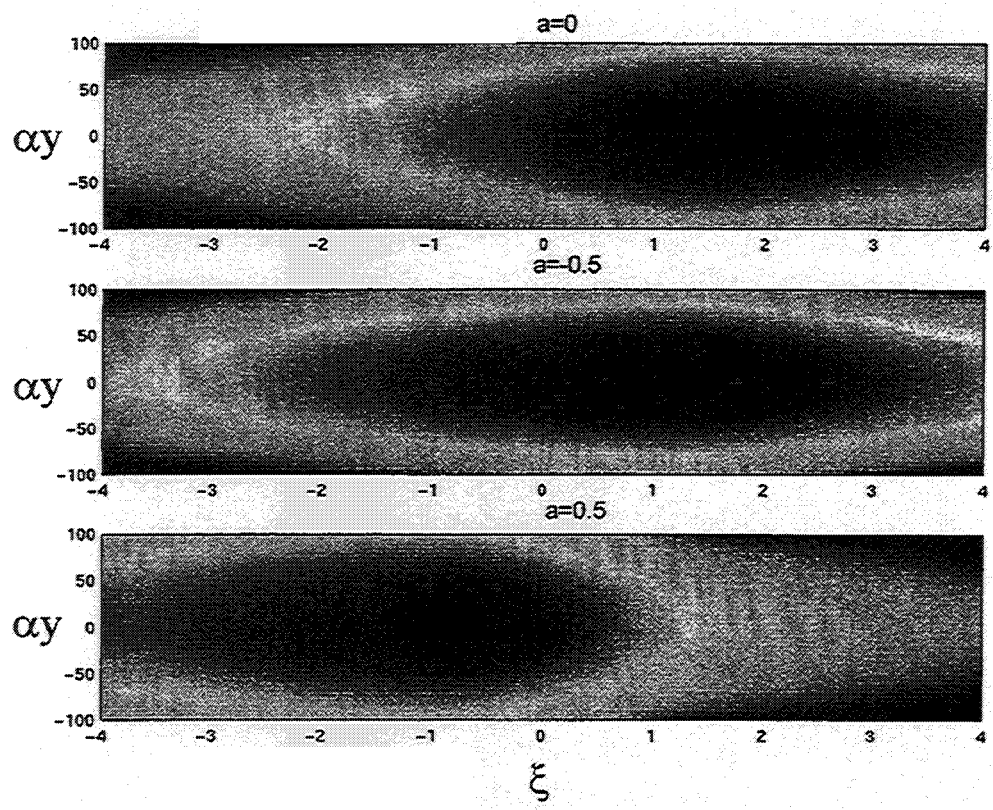


Figure 8: Streamlines and vortex location for $M = 0.2$, $M_0 = 3$, and three different values of a (0,-0.5,0.5).

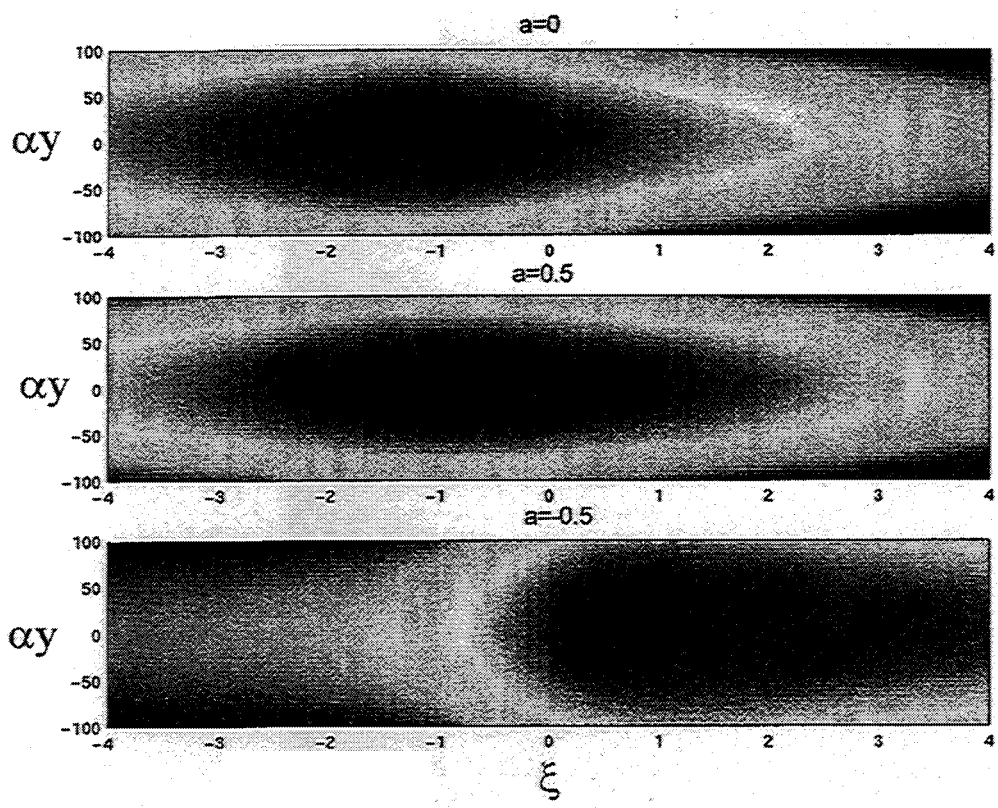


Figure 9: Streamlines and vortex location for $M = 5$, $M_0 = 10$, and three different values of α (0, -0.5, 0.5).

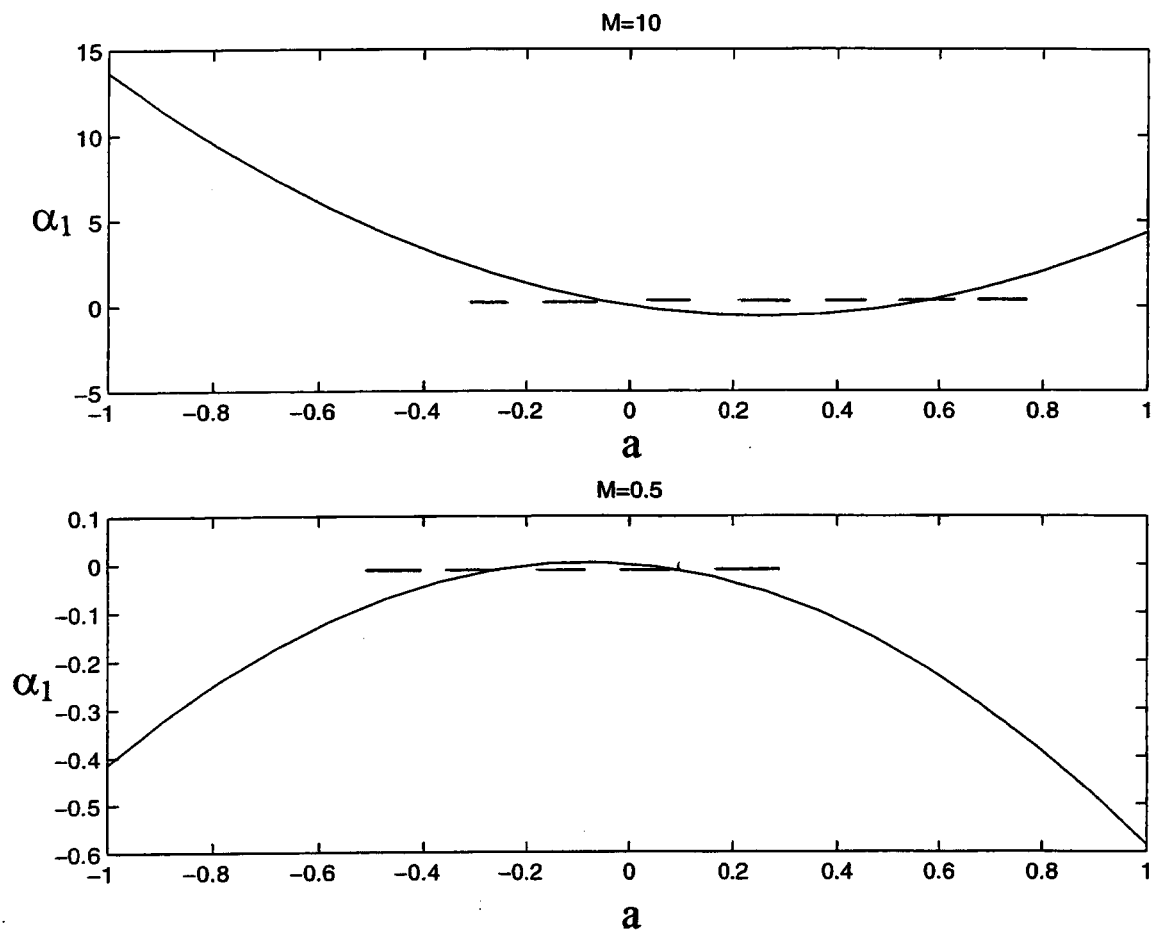


Figure 10: Effect of the heterogeneity parameter a on the onset of instability in the presence of gravity, under conditions of a homogeneous neutrally stable displacement: (a) End-point viscous unstable ($M = 10$), (b) end-point viscous stable ($M = 0.5$).

